Experimental study of the frost formation on the cryogenic flat plate with temperature distribution

Kiyoto Fujimatsu, Nobuhiro Tanatsugu, Tetsuya Sato
University of Tokyo Department of Aeronautics and Astronautics
3-1-1, Yoshinodai, Sagamihara, Kanagawa 229-8510 Japan
fujimatsu@pub.isas.ac.jp

Keywords: pre-cooler, frost formation

Abstract

In this study, a fundamental experiment was carried out to investigate the frost formation on a cryogenic flat plate with/without temperature distribution from 230K to 160K under the convective flow. The effects of mixing ethanol as a condensable substance were also researched. From the test results, when surface temperature at the upstream is 230K, mass flux is high. On the other hand, when surface temperature at the downstream is 160K, mass flux is low. The degree of improvement to restrain frost formation by ethanol mixing is relatively larger at the upstream than at the downstream.

1. Introduction

The development of ATREX engine (Air Turbo Ramjet engine with EXpander cycle) has been engaged for years as a candidate for the fly back booster of the reusable TSTO space plane. It aims to accelerate up to Mach 6 at an altitude of 30 km.

Fig.1 shows a flow diagram of the ATERX engine. a) The air is taken in at the air-intake. b) It is cooled at the pre-cooler. c) It is compressed at the fan. d) It is mixed with the fuel hydrogen at the mixer. e) The mixed gas is burned at the combustion chamber. f) The combustion gas is exhausted from the plug nozzle. In these components of this engine, the pre-cooler is a cryogenic heat exchanger, which cools down the incoming airflow by using fuel liquid hydrogen as a coolant. Pre-cooling the air gives some benefits, that is, decrease of thermal load to the fan to expand the flight range, and decrease of compressive work at the fan to increase the thrust and specific impulse. On the other hand, it is the most severe problem that thick frost formation occurs, when moist air is exposed to a cold surface (Fig.2).
It causes the aerodynamic problem such as increase of pressure drop of the airflow, and the thermodynamic problem such as decrease of heat transfer rates.

In this paper, the results of firing test under the sea level and the frost formation on a cryogenic flat plate with/without temperature distribution from 230K to 160K are referred.

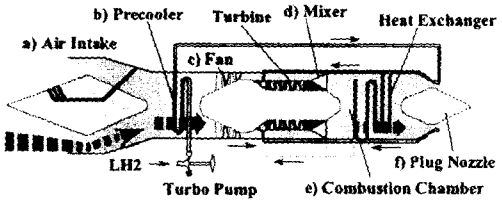

Fig.1 ATR engine with Expander cycle

2. Frost formation

2.1 Frost formation and Mist

Frost formation is a phenomenon that the water vapor in the air is sublimated or condensed on the cold surface. Sometimes the water vapor in the air changes the phase to minute droplets in the boundary layer. These droplets are called mist. According to the previous studies [1-2], the mass flux of mist is lower than that of water vapor.

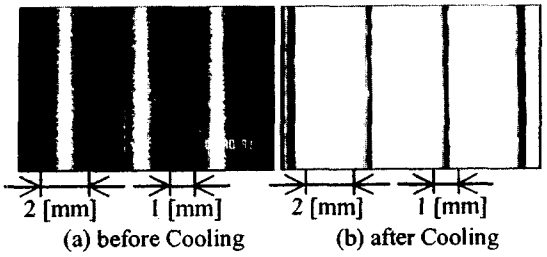

Fig.2 Frost formation

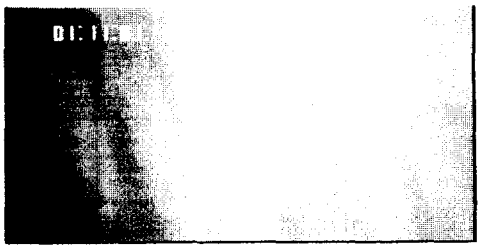

Fig.3 Frost formation on the inner tubes

2.2 Defrosting method

Against this problem, an innovative method was proposed, that is to mix the condensable gas such as methanol in the air, and its effect was examined by using a sub-scale heat exchanger model. The gas flows into the frost layer, and is sublimated or condensed with water vapor on the cold surface. As a result of this, it is expected to increase the frost density, and decrease the thermal resistance.

According to the previous studies[3], pressure loss could decline by mixing just a small quantity of the condensable gas as much as the water vapor.

3. Firing test under the sea level

Firing test of the ATREX engine was carried out last year to prove the effect of mixing methanol as the condensable substance.

(a) In case of mixing methanol in the liquid phase, the water vapor changes phase to mist, and surplus methanol is frost or ice on the cryogenic surface.

(b) According to the previous studies[4], in case of mixing methanol in the gas phase, surplus methanol was hard to change the phase to frost.

From these concepts, firing test was carried out in the following two mixing way.

1) Pneumatic spray type: Spraying minute particles of methanol in the liquid phase, whose diameter is about 10 μm.
2) Gaseous-type: Mixing the methanol vapor.

From the test results, we could succeed in deceasing the pressure loss throughout the firing test. But the frost formation on the inner tubes was still observed. (Fig.3, Fig.4)

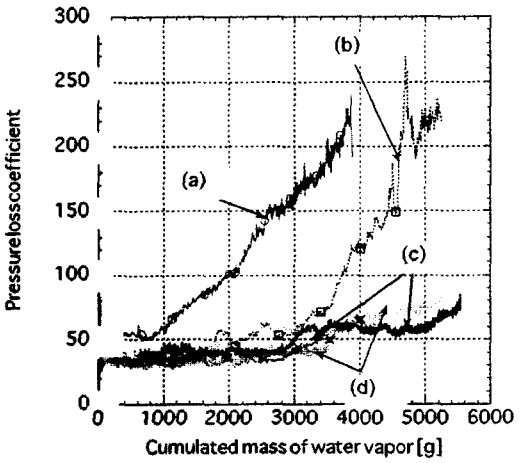

Pressure loss coefficient
$$= \frac{\text{Pressure loss between pre-cooler inlet and outlet}}{\text{Dynamic pressure at the pre-cooler inlet}}$$

(a) Only water vapor
(b) Collision-type(particle diameter is 10(μm～)
(c) Pneumatic spray-type
(d) Gaseous-type

Fig4 Firing test result of ATREX14

4. Research purpose

On the cryogenic surface such as the pre-cooler, the frost formation is caused by not only mass transportation of water vapor but that of mist. Therefore, the frost formation at the upstream differs from that at the downstream due to the difference on the air temperature.

In this study, it is the purpose to acquire the fundamental understanding of the frost formation on the cryogenic surface with/without temperature distribution. The effects of mixing ethanol as a condensable substance were also researched. Though

the actual pre-cooler is composed of circular tube banks, this experiment was carried out for a flat plate, because it simplifies the phenomenon.

5. Experimental apparatus

Fig.5 shows the experimental apparatus used in this study. It is composed of four sections:

(a) The reservoir section:

A polyethylene bag (The volume is almost 3[m^3].)

The humidity and temperature of the inlet air were measured by a thermo-hygrometer.

(b) The cooling section:

Copper plates, attached to sidewalls of the test section, were dipped in liquid nitrogen in a storage box made of foam polystyrene. Thus the sidewalls, which were used as the cooling surfaces, were cooled down by thermal conduction. The temperature of the sidewalls was controlled by changing the position and the number of copper plates.

(c) The test section:

Both sidewalls made of copper (length of 500mm, height of 100mm and thickness of 5 mm) are the cooling surfaces.

At this section, the temperature of main flow and walls were measured by type-K thermocouples. The velocity of main flow was measured by a hot-wire anemometer.

The difference pressure of main flow between inlet and outlet, was measured by a pressure transducer.

The image was recorded by a CCD-camera.

(d) The blower section:

An electric blower was used.

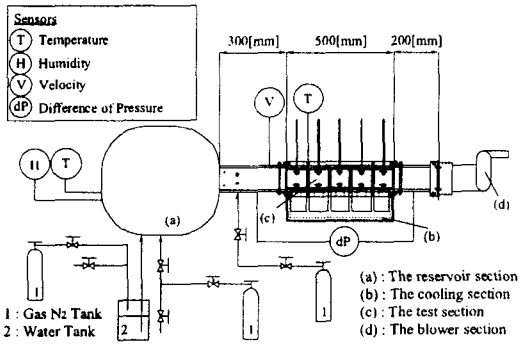

Fig.5 Schematic of the experimental apparatus

6. The method of simple calculation

According to the previous studies[2-4], mass flux of water vapor to the frost surface is determined by convective diffusion from the main flow to the frost surface.

$$\dot{m}_v = \rho_a \times h_D \times \left(W_v(T_\infty) - W_{vsat}(T_{fs})\right) \tag{1}$$

Mass transfer coefficient h_D is determined by the following equation by using the local Sherwood number Sh_x.

$$h_D = Sh_x \times \frac{D}{x} \tag{2}$$

This test section has a 100mm × 10mm cross section, which is similar to the phenomenon on a single flat plate. Though hydrodynamic boundary layer develops from the top of the test section, thermal boundary layer develops from the distance of 300mm from the top of the test section. (Fig.6)

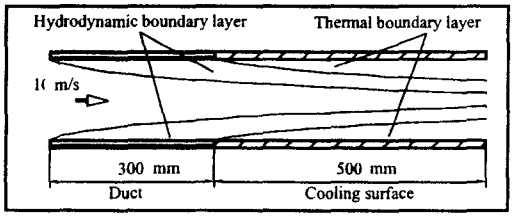

Fig.6 Boundary layer

In this study, the following formula proposed by Reynolds et al.[5] was used with respect to heat transfer.

Through analogy between heat and mass transfer, local Sherwood number was given.

$$Nu_x = 0.0296 \times \mathrm{Pr}^{\frac{3}{5}} \times \mathrm{Re}_x^{\frac{4}{5}} \times \left[1 - \left(\frac{0.3}{x}\right)^{\frac{9}{10}}\right]^{\frac{1}{9}} \quad (3)$$

$$Sh_x = 0.0296 \times Sc^{\frac{3}{5}} \times \mathrm{Re}_x^{\frac{4}{5}} \times \left[1 - \left(\frac{0.3}{x}\right)^{\frac{9}{10}}\right]^{\frac{1}{9}} \quad (4)$$

The frost surface temperature was calculated on the assumption that the sum of the sensible heat transfer rate q_i and the latent heat transfer rate q_i' equal the heat transfer rate on the cooling wall q_i''.

Energy balance

$$q_i'' = q_i + q_i' \quad (5)$$

Sensible heat transfer rate : q_i

$$q_i = (\dot{m}_a \times Cp \times T_a)_{i+1} - (\dot{m}_a \times Cp \times T_a)_i \quad (6)$$

Latent heat transfer rate : q_i'

$$q_i' = \dot{m}_v \times i_{sg} \quad (7)$$

Heat transfer rate on the cooling wall : q_i''

$$q_i'' = \lambda_{eff} \times \frac{T_{fs} - T_{Wi}}{\delta_f} \times S \quad (8)$$

Here, λ_{eff} is effective thermal conductivity in the frost layer, the following correlation proposed by Lee et al.[6-7] was used. δ_f is the thickness of the frost layer, which was estimated by the image captured by a CCD camera.

$$\lambda_{eff} = 0.132 + 3.13 \times 10^{-4} \cdot \rho_f + 1.6 \times 10^{-7} \cdot \rho_f^{\,2} \quad (9)$$

7. Experiment

7.1 In case of only water vapor

7.1.1 Procedure

1) Before starting frosting experiment, to prevent frost formation, duct was filled with dry nitrogen gas.
2) The reservoir was filled with the dry nitrogen gas and controlled the humidity by spraying water.
3) The flat plates were cooled to achieve the experimental condition.
4) After finishing frosting experiment, the frost was gathered into sampling cases and weighed.

7.1.2 Test conditions

Test conditions are listed at Table.1, and temerature distribution on the cooling wall in case of (b) is shown at Fig.7.

Table.1 Test conditions

Main flow velocity:	10	m/s
Water vapor mass fraction:	6.5	g/kg
Test duration :	200	sec
Temperature of cooling wall		
(a) Temperature of cooling wall is uniform.		
	240, 190, 120	K
(b) Temperature of cooling wall is distributed.		
From	230 (upstream)	K
To	160 (downstream)	K

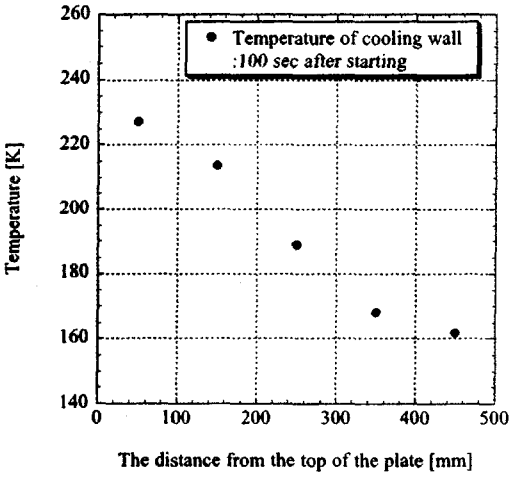

Fig.7 Temperature distribution

7.1.3 Test results

1) Uniform temperature of wall: 240K

Frost formation occurred all over the cold surface (Fig.9). Mass flux at the upstream was higher than that at the downstream.

Mass flux by experimental data agreed with that predicted by the simple calculation (Fig.8).

The further the distance from the top was, the lower

mass flux was. This was shown in the following reason. Mass flux by vapor diffusion was in proportion to the mass fraction gradient between the wall and its surroundings. The concentration boundary layer at the downstream was thicker, and the mass fraction gradient became smaller than at the upstream. As a result, the mass flux became lower at the downstream.

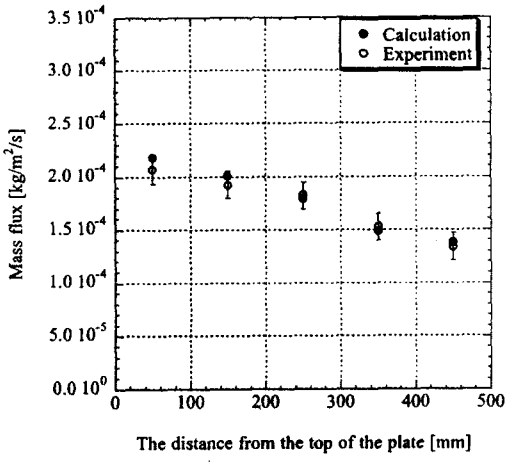

Fig.8 Mass flux: 240K

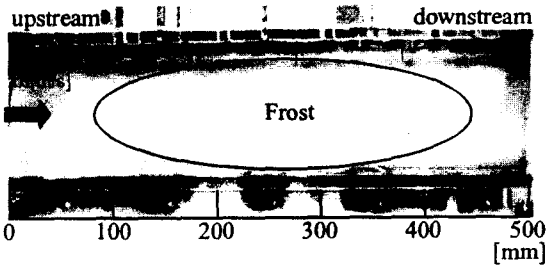

Fig.9 Photograph of the frost formation: 240K

2) Uniform temperature of wall: 190K

Frost formation occurred at the upstream. It was observed that the frost attaching to the surface was blown off at the midstream (Fig.11) and mist flow occurred (Fig.12).

Compared with the calculation, mass flux by experimental data agreed with the calculation at the upstream, but mass flux by experimental data was lower than the calculation at the midstream and downstream (Fig.10). According to the previous studies[1-3],

1) Frost generated from mist is low density, easy to be blown off.

2) Mass flux of mist is lower than that of vapor.

From these facts, the decrease of mass flux was mainly caused by mist formation and blowing of the frost.

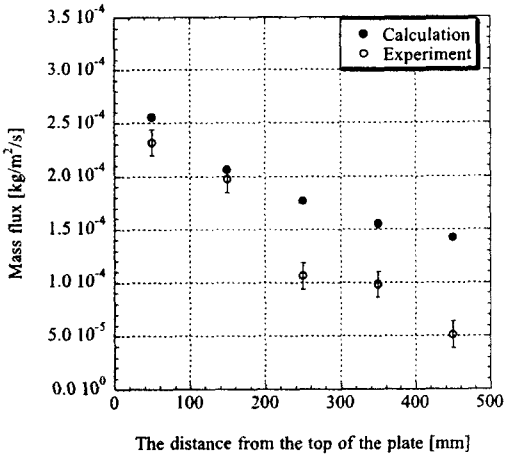

Fig.10 Mass flux: 190K

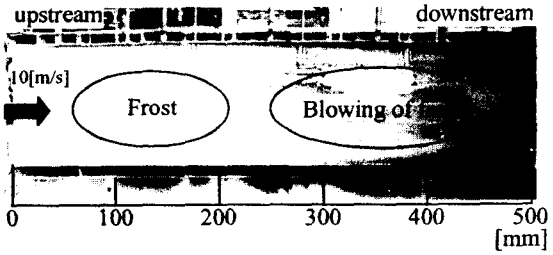

Fig.11 Photograph of the frost formation: 190K

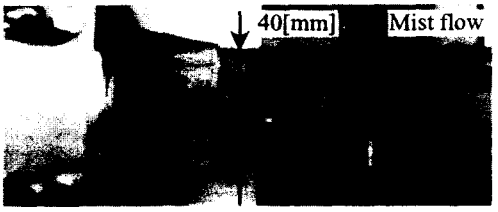

Fig.12 Photograph of mist flow at the duct outlet

3) Uniform temperature of wall: 120K

It was observed that the frost attaching to the surface was blown off at the top of the plate (Fig.14), and mist flow occurred.

Mass flux by experimental data at a distance of

50mm from the top was a little larger than others in Fig.13. This was because the boundary layer was thin at the top of the plate, then vapor was transported without changing the phase to mist, thus the mass transportation by vapor diffusion was more dominant than that of mist. Altogether, mass flux by experimental data was lower than the calculation (Fig.13). As mentioned above, the decrease of mass flux was mainly caused by mist formation and blowing of the frost.

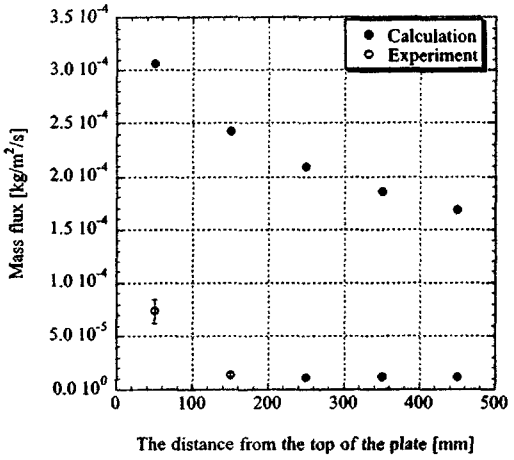

Fig.13 Mass flux: 120K

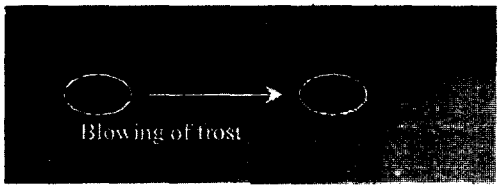

Fig.14 Magnified photograph at the top: 120K

4) Temperature distribution: from230K to160K

It was observed that the frost attaching to the surface was blown off at the midstream, and mist flow occurred (Fig.16).

Experimental data was close to the calculation at the upstream, but it was much lower than the calculation at the midstream, and downstream (Fig.15).

From the test results of the uniform temperature, water vapor diffusion was dominant to mass transfer at the upstream, but mass flux decreased at the midstream and downstream because of mist formation and blowing of the frost.

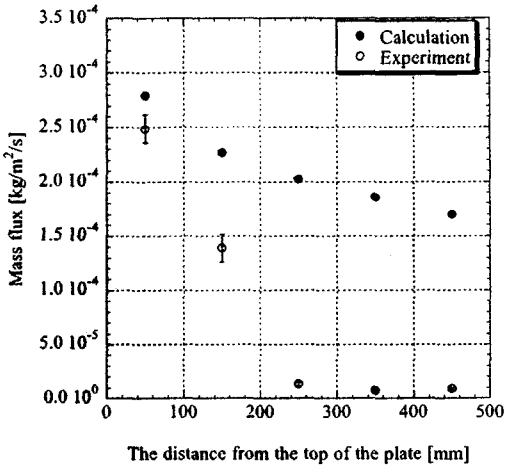

Fig.15 Mass flux

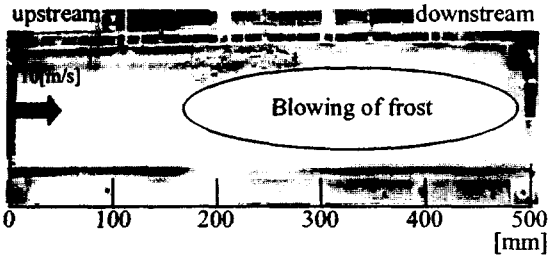

Fig.16 Photograph of the frost formation

7.2 In case of mixing ethanol vapor

7.2.1 Procedure

1) Before the experiment, to prevent frost formation, duct was filled with dry nitrogen gas.
2) The reservoir was filled with the dry nitrogen gas and controlled the humidity by spraying mixed solution.
3) The flat plate was cooled to achieve the experimental condition.
4) After finishing a blow, the frost was gathered into sampling cases and weighed. Besides this, a ratio of ethanol in the frost was measured after melted.

7.2.2 Test conditions

Test conditions are listed at Table.2.

Table.2 Test condition

Main flow velocity:	10	m/s
Water vapor mass fraction:	6.5	g/kg'
Ethanol vapor mass fraction:		
	3.5, 6.5, 7.5	g/kg'
Test duration:	200	sec
Temperature of cooling wall is distributed.		
From	230 (upstream)	K
To	160 (downstream)	K

7.2.3 Test results

The following phenomenon was observed in case of mixing ethanol vapor.

(a) At the upstream (Fig.18)

Condensed liquid was attached to the cooling wall.

(b) At the midstream (Fig.19)

Condensed liquid and frost were attached to the cooling wall.

(c) At the downstream (Fig.20)

Frost was attached to the cooling wall.

Fig.21 shows the mass ratio of ethanol in the frost.

In terms of the mass ratio of ethanol, obvious differences among the measuring positions were not found.

This phenomenon was true for other results measured under the different initial condition.

It was predicted that the water vapor and ethanol were not separately transferred but together as if they had been the pure substance. As a result, when the temperature of cooling wall was near the melting point of mixed liquid, condensed liquid attached to the cooling wall.

When the wall temperature was below the melting point, frost attached to the cooling wall.

(The melting point of mixed liquid was about 234K.)

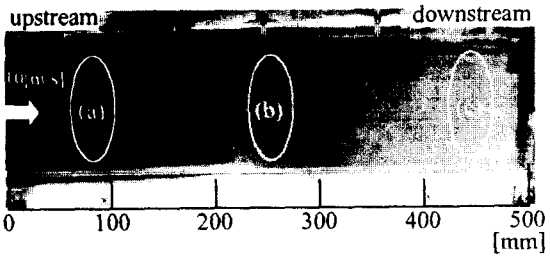

Fig.17 Photograph of the frost formation

Fig.18 Magnified photograph at the upstream

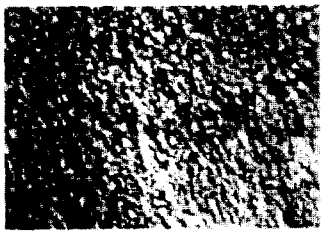

Fig.19 Magnified photograph at the midstream

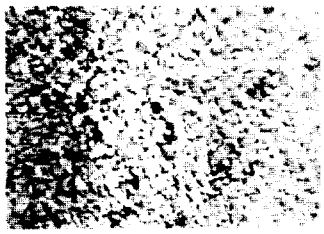

Fig.20 Magnified photograph at the downstream

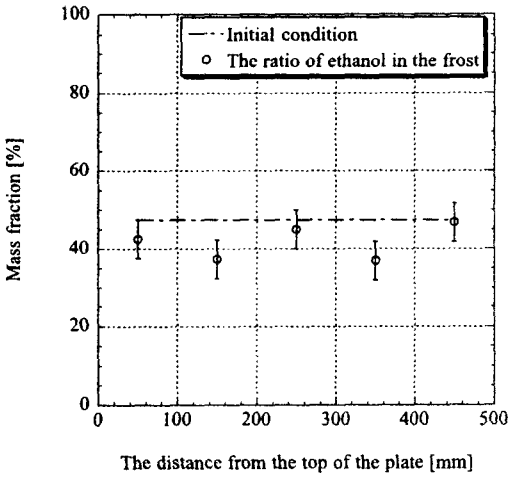

Fig.21 The ratio of ethanol of the frost

8. Conclusion

In this study, the following phenomena on the frost formation on a cold flat surface were made clear,

1) Mass flux by vapor diffusion considering of mist formation is lower than that by vapor diffusion without considering of mist formation.
2) On the cryogenic flat plate with temperature distribution from 230K to 160K, mass flux at the upstream is high, mass flux at the downstream is low because of mist formation and blowing of frost.
3) In case of mixing ethanol vapor on the cryogenic flat plate with temperature distribution from 230K to 160K, condensed liquid was attached at the upstream, and frost was attached at the downstream. From this result, the inhibitory effect of the methanol mixing on the frost formation is larger at the upstream rather than at the downstream.

References

1) H,Ookubo; The Frosting Phenomenon to the Vertical Plate in Natural Convection Flow. *Japan society of Refrigerating*, 1983,**58**,663,3-11
2) 原田賢哉:極低温冷媒を用いた空気熱交換機の着霜に関する研究, 1999 東京大学博士論文
3) 木村竜也:プリクーラの着霜に関する研究, 2000 東京大学修士論文
4) 坪本卓:凝縮性物質の液相混入によるプリクーラの着霜低減に関する研,2002.東京大学修士論文
5) 伝熱工学資料, 日本機械学会, 東京, 1997,44-49
6) K.S. Lee, Prediction of the frost formation on a cold flat surface, *International Journal of Heat and Mass Transfer*, 2003,**46**,3789-3796
7) K.S. Lee, A one-dimensional model for frost formation on a cold flat surface, *International Journal of Heat and Mass Transfer*, 1997,**40**,18,4359-4365

APPENDIX

Nomenclature

C_p	Specific heat [kJ/kg/K]
D	Diffusion coefficient [m^2/s]
h_D	Mass transfer rate [m/s]
i_{sg}	Latent heat [J/kg]
$\dot{m}_v$	Mass flux of vapor [kg/m^2/s]
$\dot{m}_a$	Mass flow rate of main flow [kg/s]
q	Sensible heat transfer rate [W]
q'	Latent heat transfer rate [W]
q''	Total heat transfer rate [W]
S	Heat transfer area [m^2]
T_w	Temperature of wall [K]
T_{fs}	Temperature on frost surface [K]
T_a	Temperature of main flow [K]
W_v	Mass fraction of vapor [g/kg]
W_{vsat}	Mass fraction of saturated vapor [g/kg]
x	Distance from the top of the test section [m]
δ_f	Frost thickness [m]
λ_{eff}	Effective thermal conductivity [W/m/K]
ρ_a	Density of main flow [kg/m^3]
ρ_f	Density of main frost [kg/m^3]

Nu_x	Local Nusselt number
Pr	Prandtl number
Re_x	Local Reynolds number
Sc	Schmidt number
Sh_x	Local Sherwood number

Subscripts

i	index